Mechanics of Advanced Composite Structures

Journal homepage: https://macs.semnan.ac.ir/

Semnan University

ISSN:2423-7043

Research Article

Lattice Structure Optimization of 3D Printed TPMS under Different Loading Conditions Using Regression Machine Learning

Rakesh Motgi[a], Vijay Kumar Jatti[b], Shahid Tamboli[c*], Javed Dhalait[d]

[a] *Department of Mechanical Engineering, A. G. Patil Polytechnic Institute, Solapur, 413008, Maharashtra. India*
[b] *Department of Mechanical Engineering, Bennett University, 201310, Greater Noida India*
[c] *Department of Mechanical Engineering, Symbiosis Institute of Technology, Symbiosis International University, Pune, 412115, Maharashtra. India*
[d] *Department of Mechanical Engineering, A. G. Patil Polytechnic Institute, Solapur, 413008, Maharashtra. India*

ARTICLE INFO

Article history:

Received: 2024-09-25
Revised:
Accepted:

Keywords:

Fused Deposition Modeling;
Lattice structure;
PLA;
Optimization;
Taguchi Method;

ABSTRACT

Modern manufacturing techniques have been significantly transformed by additive manufacturing (AM). Because of its capabilities like customized part manufacturing and, the ability to manufacture intricate and complex parts with reduced waste of material, additive manufacturing is becoming more popular. However, the properties of the parts manufactured by this method significantly vary with the variation in process parameters. Optimizing these parameters helps to extract enhanced mechanical properties. In addition, lattice structures have created new possibilities for increasing strength while lowering part weight through optimized lattice structures. The effect of lattice structure and process parameters on the specimen made using the fused deposition method (FDM) is the major focus of this study. In this work, three distinct TPMS-base (Triply Periodic Minimal Surfaces) lattice architectures are examined for a range of layer height levels. Investigations are conducted using the L9 orthogonal array. The FDM technique uses PLA plastic filament. The Taguchi method was used for optimization, and samples were evaluated on the UTM and Izod impact testing machines. Moreover, an ML model is created by applying machine learning to the collected data. In tensile and impact test data, neural network and Gaussian process regression models showed low error rates and predicted good accuracy. The neural network model for the flexural test data showed a moderate level of accuracy, suggesting potential for improvement. The models' performance was highlighted by their low RMSE, MSE, and MAE values, which show that they can predict material properties. The overall findings indicated that layer height has less impact on tensile and flexural strength than lattice structure. In contrast to the lattice structure, layer height influences the toughness.

1. Introduction

Diverse sectors, including fiber composite materials, automotive, aerospace, marine, and medical equipment, extensively utilize 3D printing technology, known for its rapid molding capabilities. Unlike traditional manufacturing methods, 3D printing offers the benefits of creating composite models, lowering processing costs, and reducing production times [1]. In fused deposition modeling (FDM), thermoplastic polymer polylactic acid (PLA) material is widely adopted as it is a biocompatible, biodegradable, and environmentally friendly plastic material [2].

*** Corresponding author.**
E-mail address: *shahidt@sitpune.edu.in*

Cite this article as:
Rakesh Motgi, Vijay Kumar Jatti, Shahid Tamboli, Javed Dhalait,2025. Lattice Structure Optimization of 3D Printed TPMS under Different Loading Conditions Using Regression Machine Learning. *Mechanics of Advanced Composite Structures*, 12(1), pp. xx-xx
https://doi.org/10.22075/MACS.2024.39315.2050

M. Mani et al. optimized process parameters for tensile strength, hardness, and surface roughness of the 3D-printed PLA parts using Taguchi analysis [3]. Several studies have been conducted considering different parameters like nozzle temperature, layer thickness, print speed, infill density, etc., along with lattice structures. Some of the lattice structures were bio-inspired by naturally observed patterns in bamboo [4], fish scale [5], chiral, starfish [6], honeycomb [7], etc. Various mechanical properties such as compression, tensile [8][9], bending [10], etc., are tested using different methods to find optimized parameters for future applications and their investigation suggests that lattice cell structure significantly affects mechanical properties. Vladimir Shevchenko et al. suggest that (TPMS) has higher mechanical characteristics and significantly exceeds classical cellular structures [11]. In one of the studies of the structure-property relationship of cubic Bravais crystal lattices, Flavia Libonati et al. found that lattice structures behave in a way that is dominated by stretching [12]. Paweł Bogusz et al. conducted tests on five distinct stereolithography printed lattice structures and discovered that the topology and orientation of the structures had a significant impact on print quality [13]. Jozef Tkac et al. presented an experimental and numerical study on the mechanical properties and damage behavior of a **3D-printed** lattice structure made of ABS material, showing that the lattice structure behaves differently for different **densities** [14]. Ibrahim M. Alarifi et al. found enhanced flexural and tensile strength in reinforced PETG/CF polymers [15]. Atikom Sombatmai et al. examined the post-yielding and failure mechanisms of additively manufactured TPMS lattice structures for metal and found gyroid lattices absorbed the highest energy [16]. Abdulla Almesmari et al. findings suggest that unit cell length is the most significant factor for improving specific compressive modulus [17]. An innovative methodology for simulating the breakdown of 3D-printed engineering design structures was created to compare the 3D-printed PETG/CF solid structural design. In this attempt**,** Ibrahim M. Alarifi et al. determined improved yield strength by 23% [18]. Shaheen Perween et al. discovered that an essential factor in enhancing compressive strength is the density of the infill [19]. Cem Güdür et al. found that the gyroid lattice structure resulted in the maximum strength for PLA [20]. S. Higuera et al. found Sheet gyroid structures made from thermoplastic materials exhibit superior mechanical properties and energy absorption capabilities than EPS foam [21]. Ajeet Kumar et al. found the supportless lattice structure outperforms the BCC lattice and EVA foam in terms of stiffness while maintaining similar energy absorption capabilities [22]. Dawit Bogale Alemayehu et al. also found the composite TPMS gyroid lattice with excellent **energy-absorbing** properties using PLA materials [23]. Tianzhen Liu et al. observed **that** TPMS lattices exhibit multi-stage energy absorption and tunable vibration isolation performance [24]. A. Viswanath et al. presented a topology optimization method for honeycomb cells that preserved the stiffness and weight of thin-walled single-cell lattice structures while increasing their buckling resistance up to 70% [25]. Sami E. Alkhatib et al. found the topology-optimized lattice structure exhibits a very high degree of isotropy in terms of specific energy absorption under high strain rates [26]. Syed Saarim Razi et al. suggest geometry, wall thickness, and stress distribution within the gyroid structure play a crucial role in determining its fracture behavior [27]. The 3D-printed lattice structures were examined by Chiara Ursini et al. found that the layering process of filament deposition was the cause of the anisotropic behavior [28]. Yingying Xue and colleagues created, produced, and described an improved three-dimensional auxetic lattice structure with better compressive qualities [29]. According to Dogue Qin et al**.,** the TPMS-D lattice structure exhibits structural stability, energy absorption, and compression performance. When compared to the cubic lattice structure, they found that the TPMS-D lattice structure had better **load-bearing** and energy absorption capacity [30]. Hemp fiber-based honeycomb sandwich structures were employed by Sheedev Antony et al. **These** structures showed high modulus and compressive strength up to 47 MPa [31]. Ahmed Abu Sabir and colleagues' study examined the viscoelastic reaction of polymeric lattice structures generated by 3D printing. The results indicate that the lattice based on shells has the optimum capability for energy dissipation and viscoelastic behavior [32]. According to research by Victor Beloshenko et al., the gyroid architecture behaved in an isotropic way whereas the honeycomb architecture displayed anisotropic mechanical characteristics in tension and bending [33]. In their experiments with lattice cores based on BCC and ECC unit cells, Shu-Yu Jhou et al. discovered that the deformation behavior and shock absorption capacity of the 3D-printed polymeric sandwich structures were greatly impacted by the lattice core's design, which included the strut diameter, length, number, orientation, and apparent material stiffness [34]. The impact of honeycombs packed with PMI foam was examined by Leilei Yan et al. who found that the specimens' compressive strength had improved [35]. In their review, Niranjan Kumar Choudhry et al. propose that various auxetic re-entrant

structures produced using the FDM 3D/4D printing process can lead to an improvement in energy absorption performance [36]. According to George Razvan Buican, the mechanical characteristics of FFF-printed components can be enhanced by switch architectures reinforced with carbon fiber and glass fiber polymers [37]. To compare a hyperbolic chiral lattice with a BCC lattice, Qingguo He et al. created a unique hybrid metamaterial and found that it was more resistant to cyclic compressive pressures [38]. When Abdelrahman et al. compared a non-Voronoi honeycomb lattice to a Voronoi honeycomb lattice, they found enhanced mechanical properties [39]. Jacob Peloquin et al. developed a **machine-learning** model that predicted Young's modulus, yield strength, and fracture strength of the 3D printed photopolymer gyroid lattices, with R^2 values above 0.87 [40]. When Pritam Poddar et al. compared their readings to other published work on carbon fiber polymer lattice structures, they discovered outstanding relative compressive strength and modulus values for carbon composite octet truss structures made using axial lattice extrusion [41]. Adithya Challapalli et al. found a new ideal unit cell by using a dataset from FEA in machine learning, and they claimed a 300% increase in buckling load [42]. According to Rafael Santiago, the absorption rate of TPMS-based lattices that are functionally graded increased by 18% [43]. To predict the dimensional variation in parts produced through FDM 3D printing, Prairit Sharma et al. developed a **machine-learning** model. They discovered that the effect of wall thickness varied between the two materials, ABS parts had lower deviation than PLA parts, and inner diameters had higher deviation than outer diameters [44]. Murugan Jayasudha et al. discovered that the XGBoost regression model significantly outperformed linear regression, random forest, AdaBoost, and gradient boosting in terms of R-squared, RMSE, and MAE metrics when it came to accurately predicting the tensile strength of 3D printed parts [45].

After reviewing the previous work, it was felt that the Gyroid lattice structure, Cubic lattice structure, BCC lattice structure, and Honeycomb structure are extensively studied by many researchers with minor modifications. Apart from this most studies have performed only compression tests for identifying the strength of different lattice structures. The Review suggests that a concurrent study of various TPMS-based lattice structures manufactured by the FDM process is needed. This study introduces a novel lattice structure (Gyroid, Cross, and Schwarz P) optimized for additive manufacturing, which has not been previously analyzed in combination with varying layer heights. The investigation of; how layer height influences tensile, impact, and flexural properties across these complex geometries represents an innovative approach that bridges the gap between structural design and material performance. This research highlights the synergy between lattice geometry and 3D printing parameters, contributing to advancements in customized AM designs for real-world applications. In this regard, the Taguchi method and Machine learning were used to optimize the parameters. To validate the results experimental tests were carried out.

2. Materials and Methods

In this study specimens were prepared as per the ASTM standards and experiments were conducted. To conduct the experiments the following methodology was adopted starting from material selection to deciding the geometry of the lattice structure. The following subsections define the materials used for this study as well as the methods and parameters employed in specimen manufacturing. It also describes the Taguchi method as well as machine learning used in the study.

2.1. Materials

The thermoplastic polymer polylactic acid (PLA) is frequently utilized in the fused deposition modeling technique. PLA is a thermoplastic polymer composed of renewable basic resources that are biodegradable. Corn starch is fermented to make PLA. PLA is inexpensive and comes in a variety of colors. Table 1 presents PLA's characteristics [1]. For this study, PLA is preferred as it offers excellent manufacturability with good mechanical properties and lower warping during printing complex lattice structures. Compared to ABS, PLA not only offers higher stiffness and tensile strength but also provides dimensional stability.

2.2. Fused Deposition Modeling

A large range of thermo-plastics, including some industrial-grade polymers that offer strength superior to Aluminium, may be printed in three dimensions using FDM technology. A 3D printer called the Flashforge Guider-II is utilized to create specimens. Table 2 shows the important printing parameters of the 3D printer

Table 1. Properties of PLA material [1]

Melting Temperature	Glass Transition Temperature	Nozzle Temperature	Density g/cc	Shrink Rate	Tensile Strength	Hardness, Shore-D
130– 180^{0}C	60– 65^{0}C	185^{0}C	1.24 – 1.26	0.37 –0.41%	61 – 66 MPa	59 Sh D

fabrication. According to the manufacturer's catalog, the nozzle temperature is kept at 220^{0}C because any deviation from this norm could result in prints of subpar quality. Additionally, the infill density is maintained at 100% because PLA material should fill the full volume of the lattice structure. For the specimens to retain sufficient strength in their walls during testing, a shell thickness of 1.2 mm is maintained.

Table 2. Printing Parameters

Parameters	Values
Print temperature	220^{0}C
Print speed	80mm/s
Nozzle diameter	0.4 mm
Shell thickness	1.2 mm
Infill pattern	line
Infill density	100%

2.3. Lattice Structure

Gyroid, Cross, and Schwarz-P lattice structures were chosen based on their remarkable geometric properties and a broad range of applications in additive manufacturing. Triply periodic minimal surface (TPMS) structures, gyroid and Schwarz-P lattices have effective stress distribution and isotropic mechanical characteristics, which make them perfect for high-performance and lightweight designs. With its intersecting struts, the Cross lattice offers increased energy absorption capacity in addition to greater tensile and flexural strength. Their choice ensures applicability to both theoretical research and real-world scenarios in domains like biomedical, automotive, and aerospace engineering. Triply Periodic Minimal Surfaces (TPMS) surfaces have zero mean curvature at all points and repeat periodically in three dimensions. Because of their limited surface area, they have a high mechanical efficiency and are perfect for strong, lightweight lattice constructions. For use in biomechanics, aerospace, and lightweight structures, TPMS-based lattice structures are being researched extensively. For the internal structure of the specimen, cells based on the Gyroid, Cross, and Schwarz-P TPMS are chosen. One of the most well-known TPMS is the Gyroid, which is distinguished by its intricate, non-self-intersecting surfaces. Since there is no direct contact between the two distinct interwoven volumes that make up its structure, it is a bi-continuous structure. It offers harmony between fluid permeability and mechanical strength. Studies indicate that the intricate geometry of gyroid-based devices contributes to their anisotropic mechanical behavior. Unlike the Gyroid, the Schwarz-P surface has a simpler shape and splits space into two connected zones. Because of its symmetry, Schwarz-P lattice structures are well-known for their isotropic characteristics. It has low density and high mechanical rigidity. A less well-known yet intriguing minimum surface with a distinctive crisscrossing pattern is the Cross TPMS. It is a Schwarz P surface variation. It provides rigidity and high energy absorption.

Figures 1 (a), (b), and (c) show the standard specimens created as per the ASTM-D standard. Figures 2 (a) to (i), illustrate how specimens are modeled in Fusion 360 software and then transformed into STL files. Flashprint Slicing software is used to process these STL files further. Table 3 provides modeling parameters for the lattice structure.

Table 3. Modeling parameters

Parameters	Values
Lattice cell size	5mm
Cell Position	Vertical
Cell solidity	0.6
Face thickness on all sides	1 mm
Blend distance	0 mm
Surface solidity	1

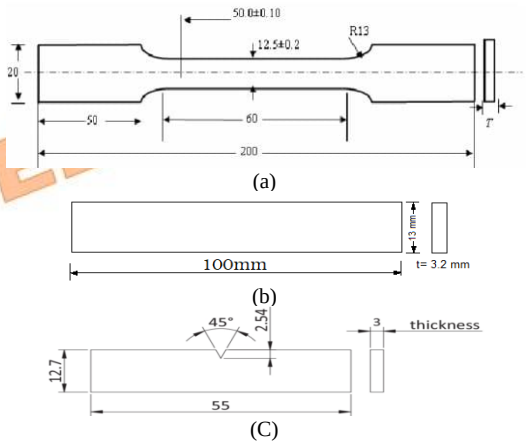

Fig. 1. (a) ASTM D638 (b) ASTM D790 (c) ASTM D256

*** Corresponding author.**
E-mail address: shahidt@sitpune.edu.in

Cite this article as:
Rakesh Motgi, Vijay Kumar Jatti, Shahid Tamboli, Javed Dhalait,2025. Lattice Structure Optimization of 3D Printed TPMS under Different Loading Conditions Using Regression Machine Learning. *Mechanics of Advanced Composite Structures*, 12(1), pp. xx-xx
https://doi.org/10.22075/MACS.2024.39315.2050

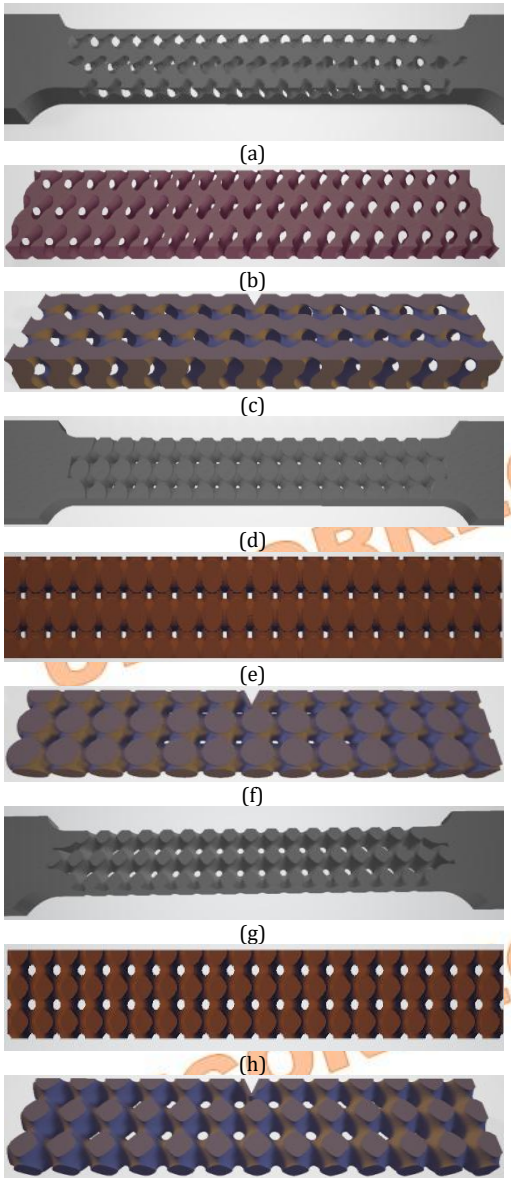

Fig. 2. STL Files (a) Tensile Test Specimen Gyroid Cell (b) Tensile Test Specimen Cross Cell (c) Tensile Test Specimen Schwarz P Cell (d) Flexural Test Specimen Gyroid Cell (e) Flexural Test Specimen Cross Cell (f) Flexural Test Specimen Schwarz P Cell (d) Izod Impact Test Specimen Gyroid Cell (e) Flexural Test Specimen Cross Cell (f) Flexural Test Schwarz P Specimen Cell

The structure in individual lattice cells has a 5 mm dimension. Cell size is typically important for balancing mechanical properties, such as stiffness and energy absorption. The orientation of the lattice cells is vertical, meaning the cell's axis aligns along the vertical direction (Z-axis) in the coordinate system. Cell orientation is important as it can influence the anisotropy of the structure. Cell solidity defines the ratio of solid material to void space within each lattice cell. A solidity of 0.6 or 60% is maintained to ensure that enough material is available to sustain various loading conditions. The intersections of the lattice structure's walls have sharp edges when the blend distance is zero. Surface solidity of 1 indicates that the external surfaces are completely solid, without any pores or voids.

2.4 Design of Experiment in Taguchi Analysis

Using Minitab, the experiment's design (DOE) was carried out. Two factors and a three-level design have been selected for Taguchi selection. The first variable is layer height, which has three levels: 0.1, 0.2, and 0.3 mm. The second variable is the selection of a TPMS-based cell, which has three levels: Gyroid, Cross, and Schwarz P. Previous work in this field served as the basis for choosing the levels. Lastly, optimization has been done to the L9 orthogonal array. Table 4 presents DOE in depth. Tensile, impact, and flexural strengths are measured on each L9 orthogonal array.

Table 4. Taguchi L9 Experimental Design (DOE)

Lattice	Layer height
Gyroid	0.1
Gyroid	0.2
Gyroid	0.3
Cross	0.1
Cross	0.2
Cross	0.3
Schwarz P	0.1
Schwarz P	0.2
Schwarz P	0.3

As per the suggested L9 array, specimens are fabricated using FDM technology. A total of 27 samples were printed and are shown in Figure 3.

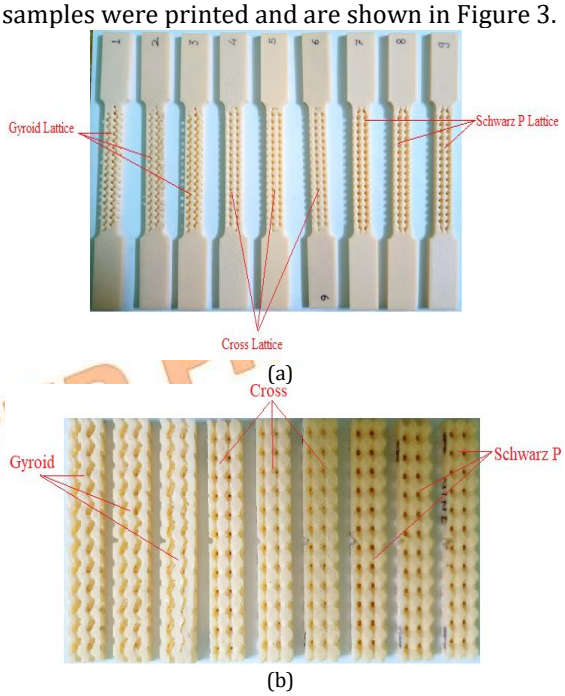

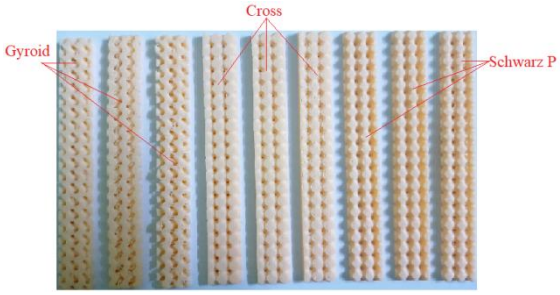

(c)

Fig. 3. (a)Tensile Test Specimens (b) Izod Impact Test Specimens (c) Flexural Test Specimens

2.5 Machine Learning

Machine learning has made it possible to recognize intricate patterns with a vast amount of data. Two types of learning can be distinguished: supervised learning and unsupervised learning. While unsupervised learning uses machine learning algorithms to analyze and cluster unlabeled data sets, supervised learning uses labeled data sets [2]. In this investigation, supervised learning is used to feed the original values. The supervised machine learning class includes the linear regression approach. The technique helps in the estimation or explanation of a particular numerical value based on a set of data. A dataset can be modeled using linear regression using the line's mathematical equation: $y = mx + c$. Building efficient models for predicting the dependent attributes from a class of attribute variables is the main goal of linear regression. Finding a positive correlation between two variables is the method's goal if they move in tandem and find a negative correlation in a case when one variable increases and the other decreases. $Y = b_0 + b_{1x}$ is the statistical equation for linear regression, where x and y are the independent and dependent variables, respectively [45]. The results obtained are used for determining the predicted values using regression learning in MATLAB.

2.6 Experimental Setup

To assess the specimens' tensile strength, elongation at break, and modulus of elasticity, tensile testing was carried out in accordance with ASTM D638. Samples in the shape of dumbbells were prepared to the standard sizes indicated in Figure 1(a) and fitted in a tensile testing apparatus. Tensile strength is measured using UTM (model No. STS 248). A constant rate of extension of 10 mm/min was applied until the specimens fractured. The tensile strength, elongation, and Young's modulus were recorded, providing critical insights into the material's ability to withstand stretching forces.

The ASTM D256 Izod impact test was utilized to evaluate impact resistance. To concentrate tension and start a fracture, specimens were prepared as indicated in Figure 1(c). After that, the samples were clamped vertically, and the notched region was struck by a pendulum swing. A one Joule hammer is used to record impact strength. By measuring the energy absorbed during fracture, the toughness and resistance to impact forces of the material were determined. Understanding plastic's behavior under abrupt loads requires the results of this test.

Similarly, a 10 kN load was applied at a rate of 5 mm/min to determine the bending stress. For this test, a three-point bending fixture is utilized. ASTM D790 was used to assess the polymers' flexural qualities. In a three-point bending test, rectangular specimens as shown in Figure 1(b) were supported at both ends and had a load applied midway with the aid of a three-point bending fixture. The specimen was loaded continuously at a rate of 5 mm/min until it either fractured or reached a predetermined limit for deflection. The stiffness and resistance to bending under the load of the material were ascertained using the obtained flexural strength and modulus values. Figure 4 (a), (b), and (c) show the setup for tensile, Izod, and three-point bending tests.

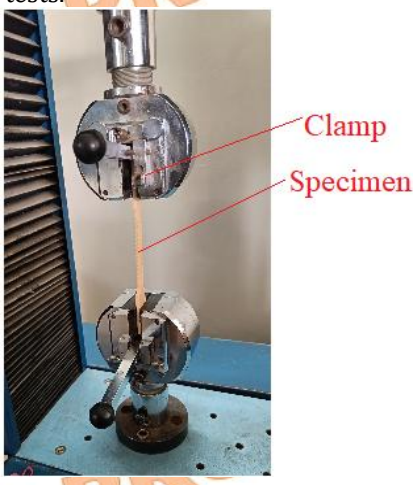

(a)

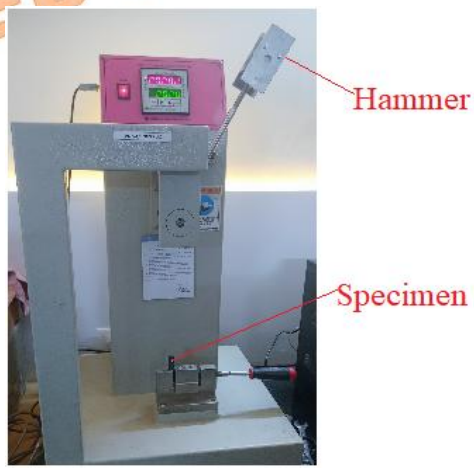

(b)

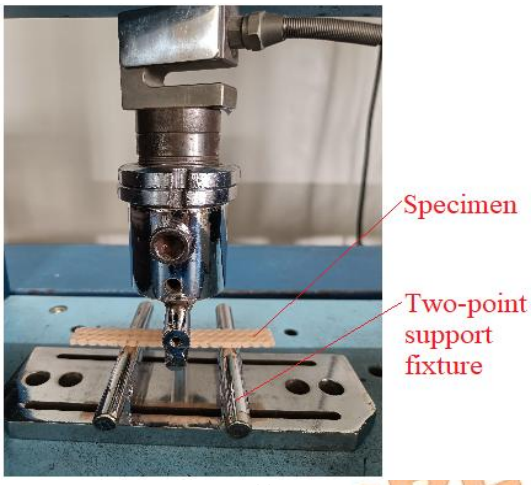

(c)

Fig. 4. (a) Tensile Test Setup (b) Izod Impact Test Setup (c) Flexural Test Setup

3. Results and Discussion

After testing the FDM 3D printed specimens for tensile, impact, and Izod tests, the following results were recorded. For a tensile test maximum stress sustained by the specimen before breaking was recorded. In the Izod test the energy absorbed as well as the impact strength of the specimen was noted down. Whereas in the flexural test by three-point bending load flexural strength was reported for each of the specimens. Table 6 shows these results.

The mechanical property data for the Gyroid, Cross, and Schwarz P lattice structures at varying layer heights are shown in Table 5. Tensile strength, impact energy, Izod impact strength, and flexural strength are among the mechanical attributes that are tested. The highest tensile strength (23.34 MPa) is found for the Cross lattice with a 0.1 mm layer height followed by Schwarz P (13.01 MPa) and Gyroid (6.23 MPa) for the same layer height.

Table 5. Test Results

Lattice	Layer height	Tensile Strength in (MPa)	Impact energy (J)	Izod impact Strength J/m	Flexural Strength (MPa)
Gyroid	0.3	5.48	0.02	3.84	13.46
Gyroid	0.2	5.9	0.08	15.3	15.38
Gyroid	0.1	6.23	0.12	23	16.02
Cross	0.3	16.23	0.04	7.6	41.66
Cross	0.2	21.43	0.1	19.2	41.34
Cross	0.1	23.34	0.13	25	48.39
Schwarz P	0.3	9.72	0.04	7.6	26.6
Schwarz P	0.2	10.79	0.07	13.4	28.84
Schwarz P	0.1	13.01	0.1	19.2	29.48

Comparing the values of tensile strength obtained by TPMS-based lattice structure with values obtained by BCC lattice structure [9] [20], it is found that TPMS-based lattice structure gives better tensile strength. Impact energy (0.13 J) is maximum for the Cross lattice with 0.1 mm layer height and lowest (0.02 J) for the Gyroid with 0.3 mm layer height. The gyroid has the lowest resistance (3.84 J/m) at 0.3 mm, whereas the Cross lattice with 0.1 mm layer height exhibits the maximum Izod impact strength (25 J/m), suggesting good resistance. At 0.1 mm layer height (48.39 MPa), the Cross lattice performs better than the Gyroid, which is the least effective (13.46 MPa) at 0.3 mm layer height. Generally increased strength is observed in tensile, impact, and flexural loading in all lattices when the layer height is decreased from 0.3 mm to 0.1 mm. Cross lattice is a great option for applications needing structural integrity because it performs better than the other structures in most categories, particularly in tensile, impact, and flexural strength. Gyroid lattice exhibits weaker mechanical properties, especially at greater layer heights, indicating that it might not be as appropriate for load-bearing applications, but it might still be useful for other purposes, such as lightweight design.

Analysis of this result was carried out in two ways, the first was Taguchi and the second was machine learning.

3.1. Taguchi Analysis

Minitab software is used to optimize the obtained results through Taguchi analysis. Greater S/N ratios are used under Taguchi analysis because stronger specimens were predicted. Response tables for means and signal-to-noise ratio are displayed in Tables 6 and 7, respectively. Figures 5, 6, and 7 illustrate the effects of the S/N ratio and the means for the tensile, impact, and flexural tests, respectively.

Table 6. Response Table Signal to Noise Ratio

Level	Tensile Test		Izod Impact Test		Flexural Test	
	Lattice Structure	Layer Height	Lattice Structure	Layer Height	Lattice Structure	Layer Height
1	15.36	21.85	20.87	26.95	23.47	29.06
2	26.06	20.90	23.75	23.97	32.81	28.42
3	20.90	19.58	21.94	15.64	29.03	27.82
Delta	10.70	2.27	2.88	11.31	9.33	1.24
Rank	1	2	2	1	1	2

Table 7. Response Table for Means

Level	Tensile Test	Izod Impact Test	Flexural Test

	Lattice Structure	Layer Height	Lattice Structure	Layer Height	Lattice Structure	Layer Height
1	5.870	14.193	14.047	22.400	14.95	31.30
2	20.333	12.707	17.267	15.967	43.80	28.52
3	11.173	10.477	13.400	6.347	28.31	27.24
Delta	14.463	3.717	3.867	16.053	28.84	4.06
Rank	1	2	2	1	1	2

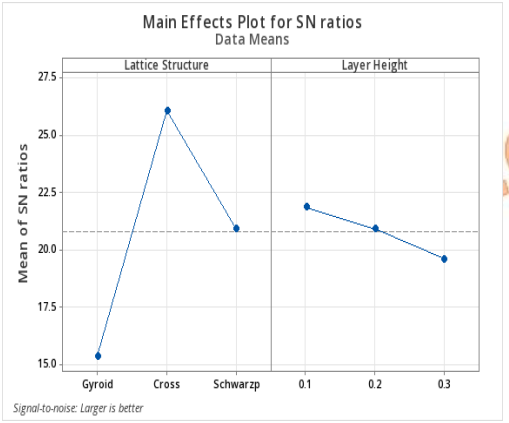

(a)

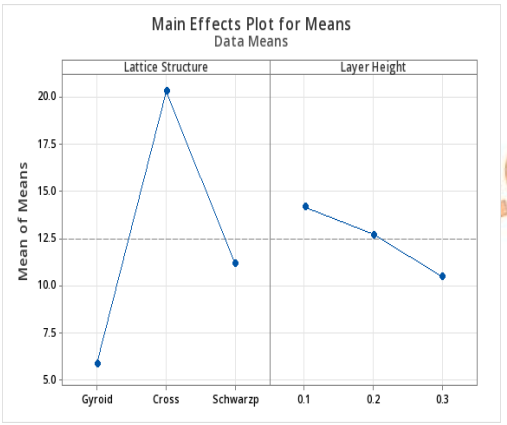

(b)

Fig. 5. (a) Main Effects of Plot for S/N ratios (b)Main Effects of Plot for Means for Tensile Test

It can be seen from Figures 5 (a) and (b), that the cross lattice has the highest mean S/N ratio, suggesting that when compared to Gyroid and Schwarz-P, this structure performs best in terms of lowering variability or enhancing robustness. The S/N ratio falls as layer height rises from 0.1 mm to 0.3 mm, suggesting that lower layer heights yield more stable and consistent structures. This is probably because fine layers will improve performance by adding more material and decreasing voids in the structure.

Figures 6 (a) and (b) reveal that the Cross structure outperforms the Gyroid and Schwarz-P structures in terms of robustness under impact loading. It does this by displaying a slightly higher mean S/N ratio.

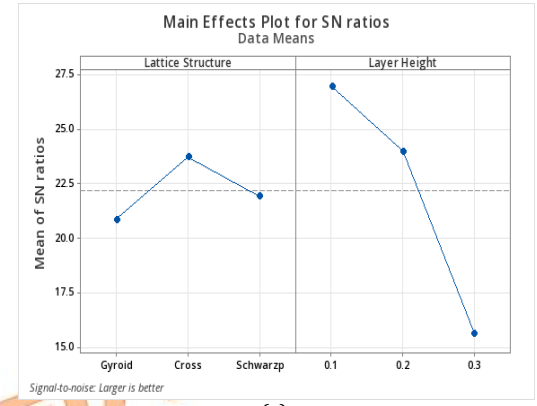

(a)

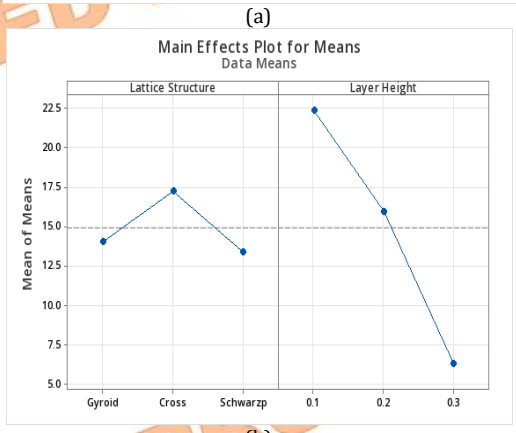

(b)

Fig. 6. (a) Main Effects of Plot for S/N ratios (b)Main Effects of Plot for Means for Impact Test

Like the results of tensile loading, in this case, the S/N ratio decreases as layer height increases, suggesting that mechanical properties will be better at lower layer heights. There is a considerable decrease in the S/N ratio as the layer height increases (to 0.2 and 0.3 mm). As a result, impact resistance varies more when layer heights are higher, probably because more voids occur. The Cross structure's superior mean performance in impact resistance highlights its appropriateness for applications requiring the absorption of energy.

The cross lattice has the largest S/N ratio, demonstrating superior performance in terms of robustness and uniformity under flexural stress, as shown in Figures 7 (a) and (b). The Gyroid structure has the lowest S/N ratio, indicating that its flexural performance may be more variable than that of the Schwarz-P structure, which displays a moderate S/N ratio. The findings support the hypothesis that lower layer heights enhance consistency and overall mechanical performance by demonstrating that a 0.1 mm layer height yields the maximum flexural strength. Larger layer heights may cause structural defects that lessen the lattice's capacity to endure loading conditions, according to all three results.

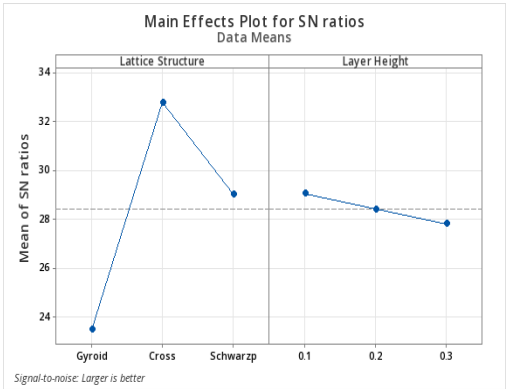

(a)

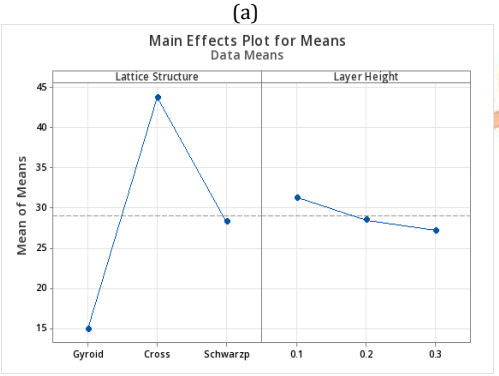

(b)

Fig. 7. (a) Main Effects of Plot for S/N ratios (b)Main Effects of Plot for Means for Flexural Test

Tables 6 and 7 present data that demonstrates the influence of lattice structure and layer height on mechanical parameters, including but not limited to tensile strength, Izod impact strength, and flexural strength. With the greatest S/N ratio and mean values in all studies, lattice structure is consistently found to be the most significant component. The level 3 lattice structure performs better than the others, demonstrating that its design maximizes mechanical strength. The material properties are mostly determined by the lattice structure, as demonstrated by the greater influence of lattice structure (Delta = 10.70 for tensile strength) over layer height (Delta = 2.27), as indicated by the Delta values. Even while layer height is secondary, it does affect performance, especially in tests of tensile and flexural strength. The study recommends concentration on lattice structure to improve the mechanical properties of materials that are 3D printed.

3.2. Analysis by Machine Learning by Using Linear Regression

MATLAB is used for determining simple linear regression models. Results obtained during the experiment are used to generate the ML model. Table 9 shows a summary of the model developed along with their accuracy.

Tensile test, Izod impact test, and flexural test results are the three types of mechanical tests for which Table 8 presents the performance of several machine learning models. Based on the unique features of each mechanical test and the advantages of each model, the choice was made to employ neural networks for tensile and flexural testing and Gaussian Process Regression (GPR) for impact testing. GPR is superior at managing uncertainty and sparsity in the highly variable and stochastic data found in Izod impact testing, but neural networks are great at collecting complicated, high-dimensional correlations in well-structured data (such as tensile and flexural tests). This customized strategy provides peak model performance and precise forecasts. The neural network model is an example of a computer model that draws inspiration from the composition and operations of the human brain. Layers of networked nodes, or neurons, make up its structure. Through training, the neurons process incoming data and identify patterns. When it comes to managing intricate, non-linear relationships in data, neural networks are very effective. For regression tasks, the Gaussian Process Regression (GPR) method yields a probabilistic, non-parametric model. It assumes that every collection of points in the input space has a joint Gaussian distribution. It establishes a distribution over functions, and conditioning this distribution on observable data allows predictions to be produced. Regression models' performance in statistics and machine learning are frequently assessed using parameters indicated in Table 8. When evaluating a model's predictive power, each indicator has a unique importance. The square root of the average squared difference between the expected and actual data is called the Root Mean Squared Error (RMSE). Larger errors are penalized more severely, and it indicates the average size of the prediction errors based on their squared values. A measure of how much of the variance in the dependent variable can be predicted from the independent variables is called the coefficient of determination, or R-squared. The average of the squared discrepancies between the expected and actual values is known as the mean squared error, or MSE. The average of the absolute discrepancies between the expected and actual values is known as the mean absolute error, or MAE. Without considering the direction of the errors, it calculates the average magnitude of errors in a series of forecasts. On the other hand, greater R-squared values suggest better accuracy.

The input layer of the trained neural network for the tensile test and the flexural test contains 2 nodes; one is categorical (lattice structure) and the other is numerical (layer height).

Table 8: Summary of the ML Models

Parameters	Tensile Test	Izod Impact Test	Flexural Test

	Neural Network (Validation)	Neural Network (Test)	Gaussian Process Regression (Validation)	Gaussian Process Regression (Test)	Neural Network (Validation)	Neural Network (Test)
RMSE	1.8381	0.00068	1.6857	0.00267	6.1058	0.42666
R-Squared	0.93	0.99	0.96	0.99	0.77	0.99
MSE	3.3786	0.00000046	2.8415	0.00000713	37.281	0.18204
MAE	1.3717	0.00053	1.3417	0.00206	5.2246	0.28444

Three fully connected hidden layers are present, with each layer containing 10 neurons. All three layers use the ReLU (Rectified Linear Unit) activation function. The output layer consists of one node having a single neuron with a linear activation function. The Gaussian Process Regression (GPR) model used for the Izod impact test employs a probabilistic approach, providing accurate predictions. A constant basis function is used to define the mean of the Gaussian process. Matern 5/2 Kernel is used to ensure flexibility and smoothness for capturing non-linear relationships in the experimental data. The isotropic kernel is used to ensure uniform scaling across all input dimensions, reducing complexity and improving generalization.

Lower MAE, MSE, and RMSE values indicate better model performance. Table 9's lower MAE, MSE, and RMSE values indicate that the model was produced with accurate performance.

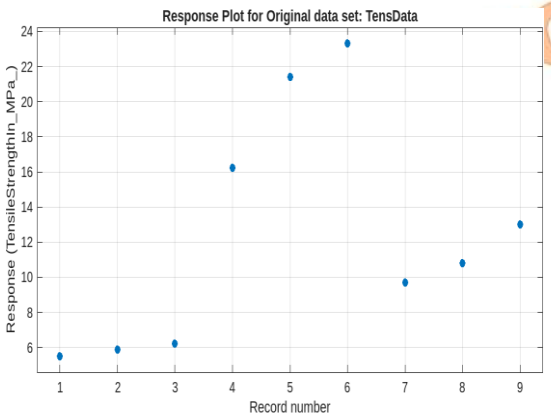

(a)

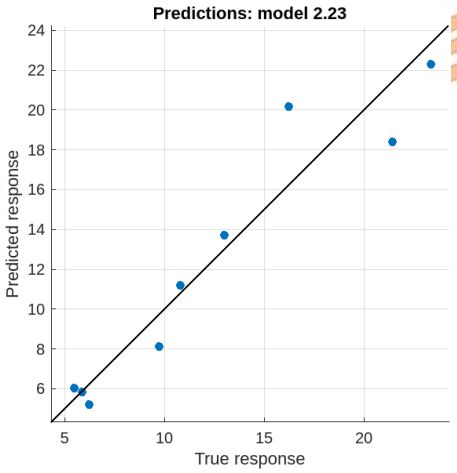

(b)

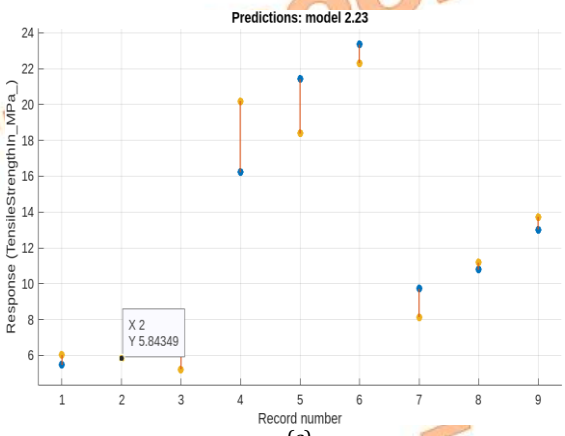

(c)

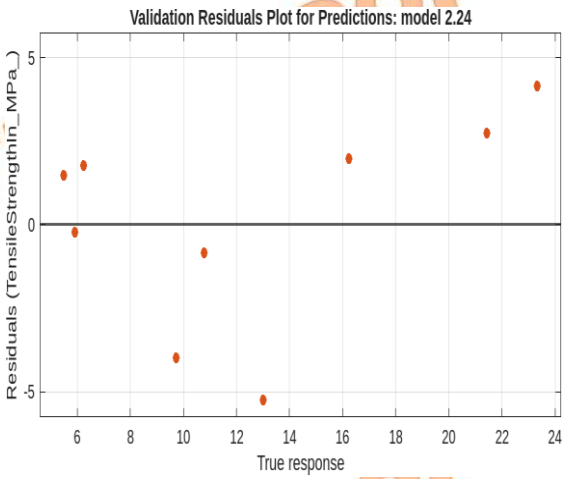

(d)

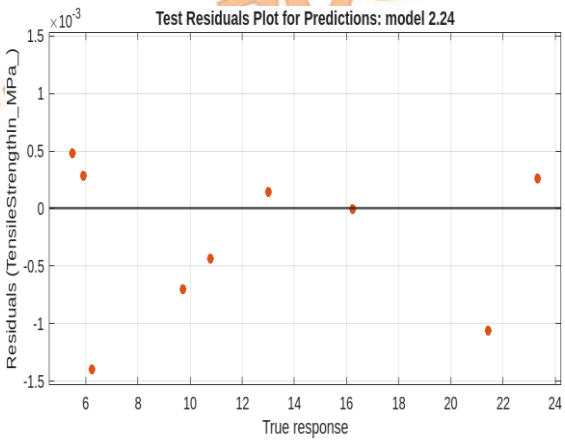

(e)

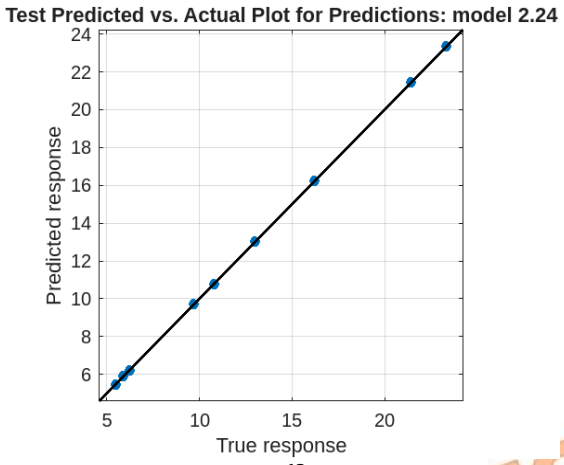

(f)

(b)

Fig. 8. Tensile Test Plots (a) Response Plot for original data set (b) Predicted Versus Actual Plot (c) Response Plot (d) Validation Residual plot for predictions (e) Test residual plot for predictions (f) Test Predicted Versus Actual Plot

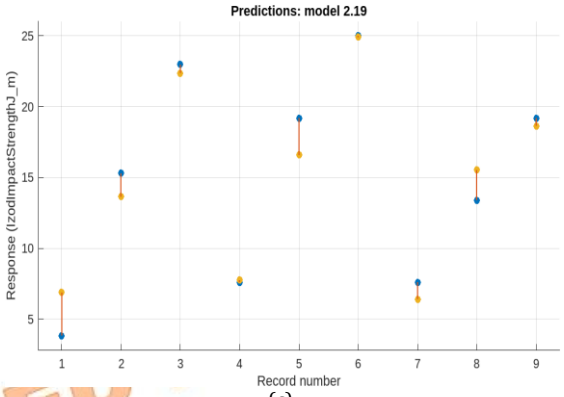

(c)

A neural network machine learning model for forecasting a material's tensile strength is demonstrated in Figures 8 (a) and (b). In Figure 8(a), the blue dots represent the actual measured tensile strengths, while the yellow points reflect the predicted tensile strengths. The difference between these points indicates the error or departure between the actual and expected values. Because most of the forecasts are within a reasonable range of the actual values, the neural network model in Figure 8(b) worked admirably. Since tensile testing measures a material's ability to withstand deformation under stress, minor errors in model prediction could result from differences in the homogeneity of the material or from external test conditions like humidity, temperature, etc., which neural networks might find difficult to fully generalize.

The Gaussian Process Regression model works exceptionally well in estimating Izod impact strength, with most of the projected values nearly matching the true values. The deviation in Figure 9(b) indicates a little tendency for the model to underestimate lower impact strength values.

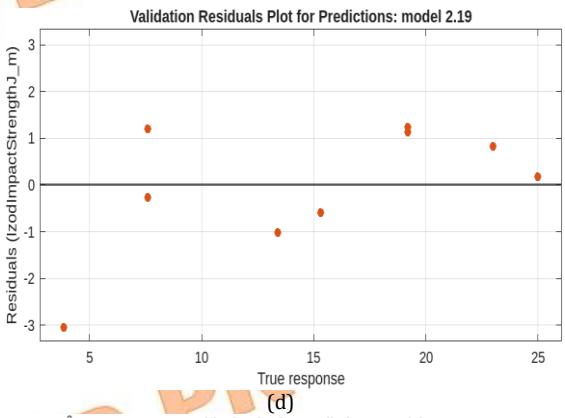

(d)

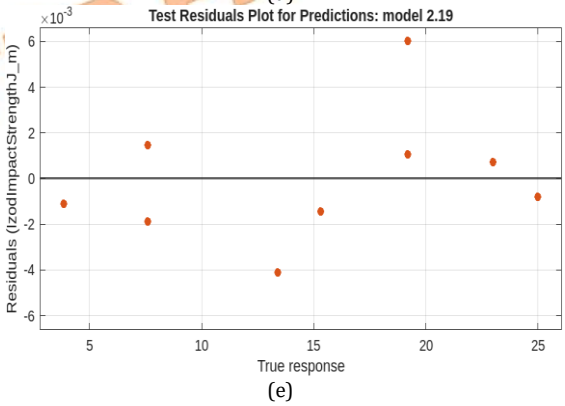

(e)

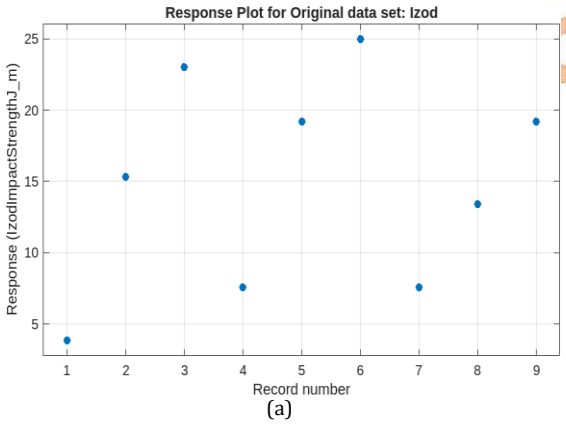

(a)

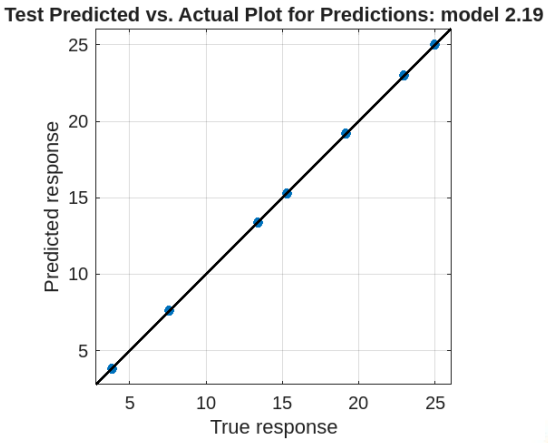

(f)

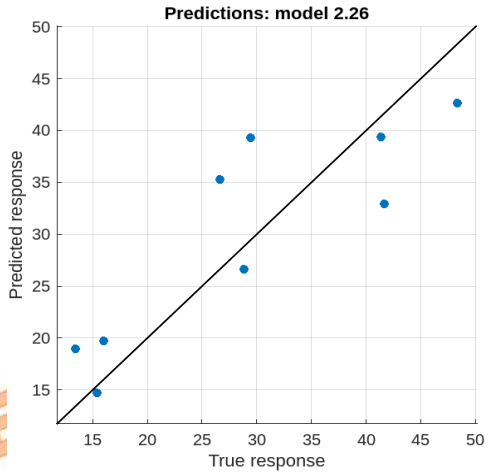

(b)

Fig. 9. Izod Test Plots (a) Response Plot for original data set (b) Predicted Versus Actual Plot (c) Response Plot (d) Validation Residual plot for predictions (e) Test residual plot for predictions (f) Test Predicted Versus Actual Plot

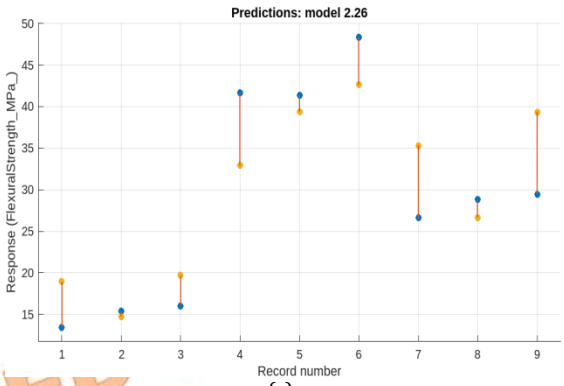

(c)

Gaussian Process Regression (GPR) performs well here, likely due to the smoothness assumption of the kernel function used (Matern 5/2). Figure 9(a) illustrates the substantial error at record 1, which may indicate anomalies in the data or a constraint in the model's ability to learn across specific impact strength ranges.

Figures 10(a) and (b) show that the neural network model has a modest level of predictive ability for flexural strength. Figure 10(b) shows a pattern of underestimate because of the model's difficulties with greater strength values, despite its accuracy for lower strength levels (below 30 MPa). The model might not generalize well over the whole dataset, especially for records with high flexural strength values, as indicated by the inaccuracies in Figure 10(a). For lower flexural strength values, the neural network model performs satisfactorily; but, for higher values, it underperforms, suggesting that the model's complexity or training data coverage may be limited.

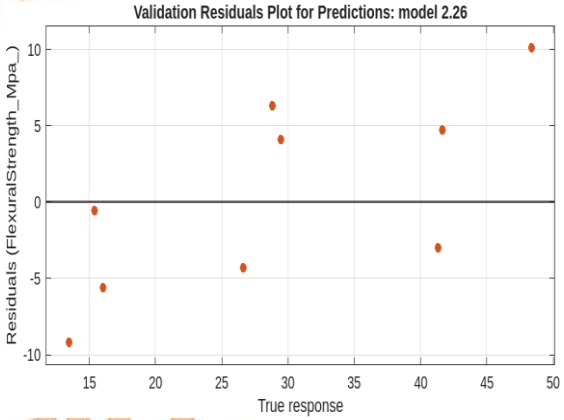

(d)

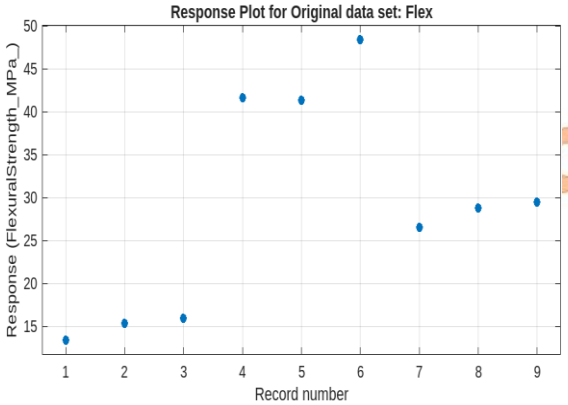

(a)

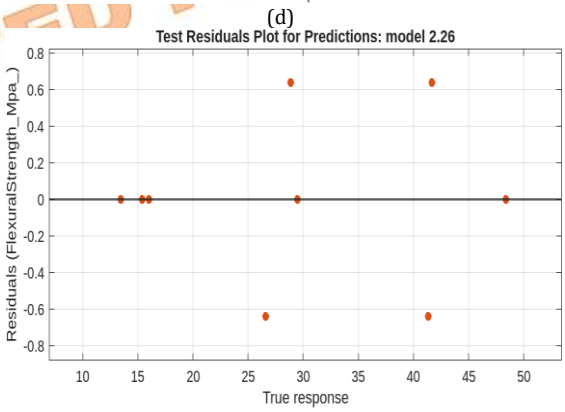

(e)

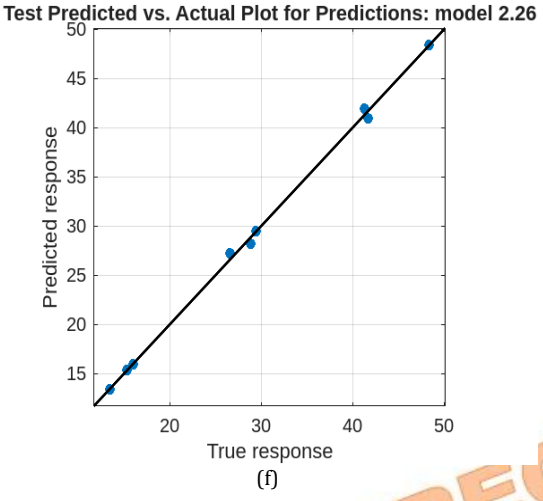

(f)

Fig. 10. Flexural Test Plots (a) Response Plot for original data set (b) Predicted Versus Actual Plot (c) Response Plot (d) Validation Residual plot for predictions (e) Test residual plot for predictions (f) Test Predicted Versus Actual Plot

Several variables, such as material stiffness, geometry, and loading circumstances, affect the flexural test, which quantifies a material's resistance to bending. Despite their strength, neural networks might find it difficult to capture these intricate relationships, which could result in increased errors.

Using strategies like dropout or L2 regularization can increase the neural network model's lower accuracy. Model performance may be improved by adjusting hyperparameters such as the number of neurons, learning rate, or activation functions. Using a larger and more varied dataset in conjunction with this training could increase the model's robustness. By machine learning standards, the dataset of nine experiments is modest, which may limit the learned models' generality and resilience. However, the existing dataset still offers useful insights because of the controlled experiments, the application of domain expertise, and the possibility of future dataset growth.

4. Conclusions

This experiment's goal was to determine how the FDM 3D printing process's lattice structure and processing settings affected the mechanical qualities of tensile strength, impact strength, and flexural strength. To optimize those properties lattice cell and layer height were the variables used for sample fabrication. Impact testing devices from Izod and UTM were used to evaluate specimen samples made from PLA. The Taguchi method was used to analyze the impacts. The results of the investigation indicated that the best combination of cross-cell and layer height, or 0.1 mm, produced the highest tensile, impact, and flexural strengths.

Tensile, impact, and flexural strength readings of 21.43 MPa, 25 J/m, and 48.39 MPa respectively provided by the aforementioned combination set are better than those of other sets of combinations. Higher Delta values and rank 1 for the tensile and flexural tests suggest that lattice structure is the more significant factor affecting the S/N ratios and the mean values. Higher Delta values and rank 1 in the Izod impact test suggest that layer height is the more significant factor affecting both the S/N ratios and the mean values.

When a neural network model was applied to tensile test data, the results showed low error rates, with an R-squared value of 0.93 indicating accuracy and low Root Mean Square Error (RMSE) and Mean Squared Error (MSE) values of 1.8381 and 3.3786, respectively. Furthermore, the model's capacity to accurately anticipate the results of tensile tests is further supported by the Mean Absolute Error (MAE) of 1.3717. When the Gaussian Process Regression model was used to analyze the data from the Izod impact test, the results showed a high degree of accuracy (R-squared = 0.96, RMSE = 1.6857, and MSE = 2.8415), indicating a low prediction error of the model. The model's accuracy in predicting the results of impact tests is shown by its MAE of 1.3417.

R-squared value of 0.77, or 77% of the variance in the flexural test data, was predicted by the neural network model. With an MSE of 37.281 and an RMSE of 6.1058, a larger prediction error is indicated. The average absolute deviation (MAE) between the predicted and actual values is 5.2246. Overall, the model shows a moderate level of accuracy, there is scope for an improvement in predicting flexural test results.

Considering the dataset's limitations, the knowledge acquired through this investigation provides a strong foundation for incorporating machine learning into workflows for materials testing and optimization. The results highlight the significance of model selection and how machine learning has the potential to revolutionize material characterization methods. By revealing hidden correlations between material compositions and performance through model training on a larger and more varied dataset, we can design high-performance PLA-based materials for use in the automotive, packaging, and medical device industries.

Funding Statement

This research did not receive any specific grant from funding agencies in the public, commercial, or not-for-profit sectors.

Conflicts of Interest

The author declares that there is no conflict of interest regarding the publication of this article.

References

[1] Tang, C., Liu, J., Yang, Y., Liu, Y., Jiang, S. and Hao, W. (2020). Effect of process parameters on mechanical properties of 3D printed PLA lattice structures. Composites Part C: Open Access, [online] 3, p.100076. doi:https://doi.org/10.1016/j.jcomc.2020.100076.

[2] Md Mazedur Rahman, Sultana, J., Saiaf Bin Rayhan and Ahmed, A. (2023). Optimization of FDM manufacturing parameters for the compressive behavior of cubic lattice cores: an experimental approach by Taguchi method. The International Journal of Advanced Manufacturing Technology. doi:https://doi.org/10.1007/s00170-023-12342-9.

[3] Mani, M., Karthikeyan, A.G., Kalaiselvan, K., Muthusamy, P. and Muruganandhan, P. (2022). Optimization of FDM 3-D printer process parameters for surface roughness and mechanical properties using PLA material. Materials Today: Proceedings. doi:https://doi.org/10.1016/j.matpr.2022.05.422.

[4] Jing, S., Li, W., Ma, G., Cao, X., Zhang, L., Fang, L., Meng, J., Shao, Y., Shen, B., Zhang, C., Li, H., Wan, Z. and Xiao, D. (2023). Enhancing Mechanical Properties of 3D Printing Metallic Lattice Structure Inspired by Bambusa Emeiensis. Materials, 16(7), pp.2545–2545. doi:https://doi.org/10.3390/ma16072545.

[5] Ramakrishna Doodi and Gunji Bala Murali (2023). Prediction and experimental validation approach to improve performance of novel hybrid bio-inspired 3D printed lattice structures using artificial neural networks. Scientific Reports,13(1). doi:https://doi.org/10.1038/s41598-023-33935-0.

[6] Namvar, N., Moloukzadeh, I., Zolfagharian, A., Demoly, F. and Bodaghi, M. (2023). Bio-inspired design, modeling, and 3D printing of lattice-based scale model scooter decks. The International Journal of Advanced Manufacturing Technology. doi:https://doi.org/10.1007/s00170-023-11185-8.

[7] Harish, A., Alsaleh, N.A., Mahmoud Ahmadein, Elfar, A.A., Djuansjah, J., Hany Hassanin, Mahmoud Ahmed El-Sayed and Essa, K. (2024). Designing Lightweight 3D-Printable Bioinspired Structures for Enhanced Compression and Energy Absorption Properties. Polymers, 16(6), pp.729–729. doi:https://doi.org/10.3390/polym16060729.

[8] Fongsamootr, T., Thawon, I., Tippayawong, N., Tippayawong, K.Y. and Suttakul, P. (2022). Effect of print parameters on additive manufacturing of metallic parts: performance and sustainability aspects. Scientific Reports, [online] 12(1), p.19292. doi:https://doi.org/10.1038/s41598-022-22613-2.

[9] Barbosa, W.S., Gioia, M.M., Temporão, G.P., Meggiolaro, M.A. and Gouvea, F.C. (2022). Impact of multi-lattice inner structures on FDM PLA 3D printed orthosis using Industry 4.0 concepts. International Journal on Interactive Design and Manufacturing (IJIDeM), 17(1), pp.371–383. doi:https://doi.org/10.1007/s12008-022-00962-6.

[10] Li, B. and Shen, C. (2022). Solid Stress-Distribution-Oriented Design and Topology Optimization of 3D-Printed Heterogeneous Lattice Structures with Light Weight and High Specific Rigidity. Polymers, 14(14), p.2807. doi:https://doi.org/10.3390/polym14142807.

[11] Shevchenko, V., Sergey Balabanov, Maxim Sychov and Lyutsiya Karimova (2023). Prediction of Cellular Structure Mechanical Properties with the Geometry of Triply Periodic Minimal Surfaces (TPMS). ACS Omega, 8(30), pp.26895–26905. doi:https://doi.org/10.1021/acsomega.3c01631.

[12] Libonati, F., Graziosi, S., Ballo, F., Mognato, M. and Sala, G. (2021). 3D-Printed Architected Materials Inspired by Cubic Bravais Lattices. ACS Biomaterials Science & Engineering. doi:https://doi.org/10.1021/acsbiomaterials.0c01708.

[13] Bogusz, P., Popławski, A., Stankiewicz, M. and Kowalski, B. (2022). Experimental Research of Selected Lattice Structures Developed with 3D Printing Technology. Materials, 15(1), p.378. doi:https://doi.org/10.3390/ma15010378.

[14] Jozef Tkáč, Samborski, S., Katarína Monková and H. Dębski (2020). Analysis of mechanical properties of a lattice structure produced with the additive technology. Composite Structures,

242, pp.112138–112138. doi:https://doi.org/10.1016/j.compstruct.2020.112138.

[15] Alarifi, I.M. (2023). Mechanical properties and numerical simulation of FDM 3D printed PETG/carbon composite unit structures. Journal of Materials Research and Technology. doi:https://doi.org/10.1016/j.jmrt.2023.01.043.

[16] Atikom Sombatmai, Krisda Tapracharoen, Vitoon Uthaisangsuk, Sabeur Msolli and Patcharapit Promoppatum (2024). Post-yielding and failure mechanism of additively manufactured triply periodic minimal surface lattice structures. Results in Engineering, [online] 23, pp.102364–102364. doi:https://doi.org/10.1016/j.rineng.2024.102364.

[17] Abdulla Almesmari, Sheikh-Ahmad, J., Jarrar, F. and Shrinivas Bojanampati (2022). Optimizing the specific mechanical properties of lattice structures fabricated by material extrusion additive manufacturing. Journal of Materials Research and Technology, [online] 22, pp.1821–1838. doi:https://doi.org/10.1016/j.jmrt.2022.12.024.

[18] Alarifi, I.M. (2023). PETG/carbon fiber composites with different structures produced by 3D printing. Polymer Testing, 120, p.107949. doi:https://doi.org/10.1016/j.polymertesting.2023.107949.

[19] Perween, S., Fahad, M. and Khan, M.A. (2021). Systematic Experimental Evaluation of Function Based Cellular Lattice Structure Manufactured by 3D Printing. Applied Sciences, 11(21), p.10489. doi:https://doi.org/10.3390/app112110489.

[20] Cem GÜDÜR, Türker TÜRKOĞLU and EREN, İ. (2023). Effect of Lattice Design and Process Parameters on the Properties of PLA, ABS AND PETG Polymers Produced by Fused Deposition Modelling. Journal of Materials and Mechatronics A, 4(2), pp.561–570. doi:https://doi.org/10.55546/jmm.1357217.

[21] Higuera, S., Miralbes, R. and Ranz, D. (2021). Mechanical properties and energy–absorption capabilities of thermoplastic sheet gyroid structures. Mechanics of Advanced Materials and Structures, pp.1–15. doi:https://doi.org/10.1080/15376494.2021.1919803.

[22] Kumar, A., Verma, S. and Jeng, J.-Y. (2020). Supportless Lattice Structures for Energy Absorption Fabricated by Fused Deposition Modeling. 3D Printing and Additive Manufacturing. doi:https://doi.org/10.1089/3dp.2019.0089.

[23] Alemayehu, D.B. and Todoh, M. (2024). Enhanced Energy Absorption with Bioinspired Composite Triply Periodic Minimal Surface Gyroid Lattices Fabricated via Fused Filament Fabrication (FFF). Journal of Manufacturing and Materials Processing, 8(3), p.86. doi:https://doi.org/10.3390/jmmp8030086.

[24] Liu, T., Zhao, W., Yao, Y., Lin, C., Zhao, H. and Cai, J. (2024). Mechanical and shape-memory properties of TPMS with hybrid configurations and materials. International Journal of Smart and Nano Materials, pp.1–25. doi:https://doi.org/10.1080/19475411.2024.2410289.

[25] Viswanath, A., Khalil, M., Khan, A., Fahad Al Maskari, Cantwell, W.J. and Khan, K.A. (2024). A novel design strategy to enhance buckling resistance of thin-walled single-cell lattice structures via topology optimisation. Virtual and Physical Prototyping, 19(1). doi:https://doi.org/10.1080/17452759.2024.2345390.

[26] Alkhatib, S.E., Xu, S., Lu, G., Karrech, A. and Sercombe, T.B. (2024). Rate-dependent behaviour of additively manufactured topology optimised lattice structures. Thin-Walled Structures, 198, p.111710. doi:https://doi.org/10.1016/j.tws.2024.111710.

[27] Syed Saarim Razi, Pervaiz, S., Rahmat Agung Susantyoko and Mozah Alyammahi (2024). Optimization of Environment-Friendly and Sustainable Polylactic Acid (PLA)-Constructed Triply Periodic Minimal Surface (TPMS)-Based Gyroid Structures. Polymers, 16(8), pp.1175–1175. doi:https://doi.org/10.3390/polym16081175.

[28] Ursini, C. and Collini, L. (2021). FDM Layering Deposition Effects on Mechanical Response of TPU Lattice Structures. Materials, 14(19), p.5645. doi:https://doi.org/10.3390/ma14195645.

[29] Xue, Y., Gao, P., Zhou, L. and Han, F. (2020). An Enhanced Three-Dimensional Auxetic Lattice Structure with Improved Property. Materials,

13(4), pp.1008–1008. doi:https://doi.org/10.3390/ma13041008.

[30] Qin, D., Sang, L., Zhang, Z., Lai, S. and Zhao, Y. (2022). Compression Performance and Deformation Behavior of 3D-Printed PLA-Based Lattice Structures. Polymers, [online] 14(5), pp.1062–1062. doi:https://doi.org/10.3390/polym14051062.

[31] Antony, S., Cherouat, A. and Montay, G. (2020). Fabrication and Characterization of Hemp Fibre Based 3D Printed Honeycomb Sandwich Structure by FDM Process. Applied Composite Materials, 27(6), pp.935–953. doi:https://doi.org/10.1007/s10443-020-09837-z.

[32] Abusabir, A., Khan, M.A., Asif, M. and Khan, K.A. (2022). Effect of Architected Structural Members on the Viscoelastic Response of 3D Printed Simple Cubic Lattice Structures. Polymers, 14(3), p.618. doi:https://doi.org/10.3390/polym14030618.

[33] Beloshenko, V., Beygelzimer, Y., Chishko, V., Savchenko, B., Sova, N., Verbylo, D., Voznyak, A. and Vozniak, I. (2021). Mechanical Properties of Flexible TPU-Based 3D Printed Lattice Structures: Role of Lattice Cut Direction and Architecture. Polymers, 13(17), p.2986. doi:https://doi.org/10.3390/polym13172986.

[34] Shu-Yu Jhou, Hsu, C.-C. and Yeh, J.-C. (2021). The Dynamic Impact Response of 3D-Printed Polymeric Sandwich Structures with Lattice Cores: Numerical and Experimental Investigation. Polymers, 13(22), pp.4032–4032. doi:https://doi.org/10.3390/polym13224032.

[35] Yan, L., Zhu, K., Zhang, Y., Zhang, C. and Zheng, X. (2020). Effect of Absorbent Foam Filling on Mechanical Behaviors of 3D-Printed Honeycombs. Polymers, 12(9), p.2059. doi:https://doi.org/10.3390/polym12092059.

[36] Choudhry, N.K., Panda, B. and Dixit, U.S. (2023). Energy Absorption Characteristics of Fused Deposition Modeling 3D Printed Auxetic Re-entrant Structures: A Review. Journal of Materials Engineering and Performance, 32(20), pp.8981–8999. doi:https://doi.org/10.1007/s11665-023-08243-3.

[37] Buican, G.R., Zaharia, S.-M., Pop, M.A., Chicos, L.-A., Lancea, C., Stamate, V.-M. and Pascariu, I.S. (2021). Fabrication and Characterization of Fiber-Reinforced Composite Sandwich Structures Obtained by Fused Filament Fabrication Process. Coatings, 11(5), p.601. doi:https://doi.org/10.3390/coatings11050601.

[38] He, Q., Hou, Y., Li, X., Li, S. and Meng, L. (2023). Investigation on the Compressive Behavior of Hybrid Polyurethane(PU)-Foam-Filled Hyperbolic Chiral Lattice Metamaterial. Polymers, 15(9), pp.2030–2030. doi:https://doi.org/10.3390/polym15092030.

[39] Abdelrahman Mohamed Ragab, Mahdi, E., Kas Oosterhuis, Dean, A. and John-John Cabibihan (2023). Mechanical and energy absorption properties of 3D-printed honeycomb structures with Voronoi tessellations. Frontiers in Mechanical Engineering, 9. doi:https://doi.org/10.3389/fmech.2023.1204893.

[40] Peloquin, J., Kirillova, A., Rudin, C., L. Catherine Brinson and Gall, K. (2023). Prediction of tensile performance for 3D printed photopolymer gyroid lattices using structural porosity, base material properties, and machine learning. Materials & Design, 232, pp.112126–112126. doi:https://doi.org/10.1016/j.matdes.2023.112126.

[41] Poddar, P., Olles, M. and Cormier, D. (2022). Mechanical Response of Carbon Composite Octet Truss Structures Produced via Axial Lattice Extrusion. Polymers, 14(17), p.3553. doi:https://doi.org/10.3390/polym14173553.

[42] Adithya Challapalli and Li, G. (2021). Machine learning assisted design of new lattice core for sandwich structures with superior load carrying capacity. Scientific Reports, 11(1). doi:https://doi.org/10.1038/s41598-021-98015-7.

[43] Santiago, R., Ramos, H., AlMahri, S., Banabila, O., Haleimah Alabdouli, Lee, D.-W., Aziz, A., Rajput, N., Alves, M. and Guan, Z. (2023). Modelling and optimisation of TPMS-based lattices subjected to high strain-rate impact loadings. International journal of impact engineering, 177, pp.104592–104592. doi:https://doi.org/10.1016/j.ijimpeng.2023.104592.

[44] Sharma, P., Vaid, H., Vajpeyi, R., Shubham, P., Agarwal, K.M. and Bhatia, D. (2022). Predicting the dimensional variation of geometries produced through FDM 3D printing employing supervised machine learning. Sensors

International,3,p.100194. doi:https://doi.org/10.1016/j.sintl.2022.100194.

[45] Jayasudha, M., Elangovan, M., Mahdal, M. and Priyadarshini, J. (2022). Accurate Estimation of Tensile Strength of 3D Printed Parts Using Machine Learning Algorithms. Processes, 10(6), p.1158. doi:https://doi.org/10.3390/pr10061158.